

- G. Kalmus, and A. Kernan, *Nuovo Cimento* **37**, 1795 (1965).
- ⁴G. D. Cable, R. H. Hildebrand, C. Y. Pang, and R. Stiening, *Phys. Rev. D* **8**, 3807 (1973).
- ⁵A. R. Clark, T. Elioff, R. C. Field, H. J. Frisch, R. P. Johnson, L. T. Kerth, and W. A. Wenzel, *Phys. Rev. Lett.* **26**, 1667 (1971); W. C. Carithers, T. Modis, D. R. Nygren, T. P. Pun, E. L. Schwartz, H. Sticker, J. Steinberger, P. Weilhammer, and J. H. Christenson, *ibid.* **30**, 1336 (1973); W. C. Carithers, D. R. Nygren, H. A. Gordon, M. L. Ioffredo, and K. W. Lai, *ibid.* **31**, 1025 (1973).
- ⁶(a) L. M. Shiraishi, thesis, University of Hawaii, 1972 (unpublished); D. B. Clarke, thesis, University of Wisconsin, 1973 (unpublished); (c) R. E. Morgado, thesis, University of Hawaii, 1973 (unpublished).
- ⁷R. J. Cence, F. A. Harris, B. D. Jones, R. E. Morgado, L. M. Shiraishi, D. E. Yount, V. Perez-Mendez, R. Van Tuyt, and D. B. Clarke, *Nucl. Instrum. Methods* **111**, 379 (1973).
- ⁸R. J. Cence, F. A. Harris, B. D. Jones, R. E. Morgado, L. M. Shiraishi, and D. E. Yount, *Nucl. Instrum. Methods* **108**, 113 (1973).
- ⁹M. W. Peters, *Nucl. Instrum. Methods* **113**, 371 (1973).
- ¹⁰The program HASH was originally written for bubble-chamber work by Robert March of the University of Wisconsin.
- ¹¹S. K. Singh and L. Wolfenstein, *Nucl. Phys.* **B24**, 77 (1970).
- ¹²R. J. Abrams, A. S. Carroll, T. F. Kycia, K. K. Li, J. Menes, D. N. Michael, P. M. Mockett, and R. Rubinstein, *Phys. Rev. Lett.* **29**, 1118 (1972).
- ¹³Particle Data Group, *Rev. Mod. Phys.* **45**, S1 (1973).

Intranuclear cascading in photographic emulsion at accelerator and cosmic-ray energies*

R. E. Gibbs

Department of Physics, Eastern Washington State College, Cheney, Washington 99004

J. R. Florian, L. D. Kirkpatrick, J. J. Lord, and J. W. Martin

Department of Physics, University of Washington, Seattle, Washington 98195

(Received 28 March 1974)

The data on the interactions of cosmic-ray protons in nuclear emulsion have been analyzed in light of the results of recent exposures of emulsion to accelerator protons. Plots of $\langle \log_{10} \tan \theta \rangle$ as a function of the number of evaporation prongs, N_h , display an energy-independent behavior which is exploited to determine the energies of cosmic-ray events. It is found that the energies quoted in the literature are generally too high. The average charged multiplicity is linearly related to N_h from 30 GeV to 5 TeV. While a model of nuclear cascading based on direct production is consistent with these data from 30 GeV to 500 GeV, a model proceeding through an intermediate state gives better agreement at cosmic-ray energies.

I. INTRODUCTION

The suggestion that the study of proton-nucleus interactions might provide insight into proton-proton processes is currently generating considerable interest.¹⁻³ It has been recognized that proton interactions in photographic emulsion are particularly useful in this regard since the observed number of heavily ionizing evaporation prongs, N_h , provides information on the number of secondary interactions occurring in the intranuclear cascade.⁴⁻⁶

In this paper we exploit this idea to compare two classes of models to the proton-emulsion multiplicity expressed as functions of N_h , atomic number A , and the primary energy E . We shall adopt the terminology of Fishbane and Trefil² in referring to the classes of models as "independent particle models" (IPM's) and "coherent production models" (CPM's). In the IPM, secondary particles

are produced directly, while in the CPM, production proceeds through an intermediate state. We have developed a simplified IPM suitable for comparison with proton-emulsion data. Gottfried's³ "energy flux cascade" (EFC) displays many CPM features and has already been cast in a form suitable for our analysis. Comparison with the Fishbane and Trefil models is possible in some instances.

Fortunately, proton-emulsion interactions exhibit some relatively simple characteristic properties which are suitable for modeling. The regularities in the accelerator data from 30 to 200 GeV are striking. It is possible to exploit these regularities to determine the energies of higher-energy cosmic-ray interactions. The cosmic-ray data analyzed in this manner are quite consistent and sufficiently accurate to provide a good test of the models in their present stage of development.

In Sec. II an examination and discussion of the relevant accelerator proton emulsion data are presented, followed by an analysis of the cosmic-ray events. In Sec. III the models are compared with the experiments.

II. ANALYSIS OF PROTON-EMULSION COLLISIONS

The data on proton collisions in emulsion have been collected from a number of sources. In our laboratory 1269 events⁷ at 30 GeV and 181 events at 200 GeV have been measured. The interactions were located by following along proton tracks. This method minimizes biases against detection of events with a small number of prongs. Tracks were classified according to the usual criterion: Tracks of greater than 1.4 times minimum ionization were classified as evaporation prongs N_h , while the more lightly ionizing tracks were classified as shower tracks⁸ n_{ch} .

The Cracow group^{9,10} has provided us with data on $\langle n_{ch} \rangle$ as a function of N_h for 675 events at 67 GeV and 999 events at 200 GeV. The proton-emulsion multiplicity has also been determined¹¹ for a sample of 5500 events at 200 GeV.

Cosmic-ray data used in our analysis include that of Lohrmann, Teucher, and Schein,¹² that of Rybicki and Wolter,¹³ the primary proton events from Barkow *et al.*¹⁴ and the ICEF collaboration,¹⁵ and the heavy primary breakup events from the ICEF¹⁶ and Brawley stacks.¹⁷ Ganguli and Malhotra¹⁸ have made a world survey of events for which $N_h \leq 2$.

A. N_h distribution

It has long been recognized¹⁹ in cosmic-ray work that the distribution of N_h values for proton-emulsion collisions depends on the primary energy only weakly, if at all. The recent accelerator results confirm this, but indicate that the percentage of $N_h=0$ events rises slowly with primary energy up to 200 GeV.¹¹ The N_h distributions in our own sample of events at 30 GeV and 200 GeV are the same within statistics and do not show this percentage rise of the $N_h=0$ events. The average values are 7.15 ± 0.21 and 7.22 ± 0.52 , respectively. The χ^2 test for the equality of the two distributions gives a value of 15.8 for 12 degrees of freedom.

For cosmic-ray interactions of greater than 1 TeV primary energy, we have calculated $\langle N_h \rangle = 6.6 \pm 0.6$.

B. $\langle \log \tan \theta \rangle$ vs N_h

Castagnoli *et al.*²⁰ have shown that

$$-\langle \log \tan \theta \rangle = \log \gamma_c, \quad (1)$$

where θ is the production angle in the laboratory and γ_c is an estimate of the Lorentz factor of the center-of-mass system. The "Castagnoli energy" is then

$$E_c = m_p (2\gamma_c^2 - 1), \quad (2)$$

where m_p is the mass of the proton and E_c is an estimate of the primary energy of the collision. However, experimentally there is a systematic difference between the logarithm of the true Lorentz factor $\gamma_{c.m.}$ and $-\langle \log \tan \theta \rangle$. Let us define this difference to be

$$f(N_h) \equiv \log_{10} \gamma_{c.m.} + \langle \log_{10} \tan \theta \rangle. \quad (3)$$

The function $f(N_h)$ represents a set of correction factors similar to those determined by Lohrmann, Teucher, and Schein.¹² In the present work, however, correction factors have been determined for each N_h value.

Empirically, we have found that our data at 30 GeV and 200 GeV can be fitted with a function of the form

$$f(N_h) = \frac{\alpha(1 + \beta N_h)}{(1 + \delta N_h)}. \quad (4)$$

The parameters of these fits along with those of a simultaneous fit to the combined data are given in Table I. These data and the best-fit curve are displayed in Fig. 1. Within the limited statistics available, the function $f(N_h)$ does not appear to depend on the energy. When averaged over the entire sample $-\langle \log_{10} \tan \theta \rangle$ is less than $\log_{10} \gamma_{c.m.}$ by 0.063 ± 0.006 at 30 GeV and by 0.044 ± 0.014 at 200 GeV.

Although better statistics and data at other energies may show $f(N_h)$ to have a weak energy dependence, a significant improvement in the estimation of the energy of cosmic-ray events can be achieved by using these correction factors.

In Table II we present energy determinations for the cosmic-ray data. Much of these data represent

TABLE I. The best fits of the data in Fig. 1 to $f(N_h)$ as given in Eq. (4).

Parameter	30 GeV	χ^2/DF	200 GeV	χ^2/DF	30 and 200 GeV	χ^2/DF
α	-0.201 ± 0.021		-0.201 ± 0.042		-0.200 ± 0.018	
β	-0.200 ± 0.016	1.9	-0.195 ± 0.055	1.8	-0.199 ± 0.014	1.7
δ	0.060 ± 0.018		0.073 ± 0.046		0.062 ± 0.016	

TABLE II. Energy determinations and the values of $\langle n_{ch} \rangle$ and $\langle N_h \rangle$ for the cosmic-ray samples.

Reference	Energy (GeV)	$\langle n_{ch} \rangle$	$\langle N_h \rangle$
12	170 ± 50	13.1 ± 0.9	8.5 ± 1.1
ICEF 348	290 ± 70	16.3 ± 2.7	9.6 ± 2.6
13	510 ± 60	19.1 ± 1.2	7.3 ± 1.0
Brawley 1115	570 ⁺⁷⁰ ₋₆₀	14.0 ± 2.7	5.1 ± 1.0
ICEF 23	2200 ⁺⁹⁰⁰ ₋₇₀₀	21.9 ± 3.8	6.0 ± 3.4
ICEF 16	2400 ⁺⁹⁰⁰ ₋₇₀₀	25.7 ± 3.1	20.0 ± 5.9
ICEF 33	4300 ⁺²²⁰⁰ ₋₁₅₀₀	21.8 ± 5.1	6.0 ± 5.5
14 and 15	4500 ⁺⁷⁰⁰ ₋₆₀₀	22.5 ± 1.4	6.1 ± 0.6
18	4700	16.3 ± 1.1	~0.8
Brawley 1010	7800 ⁺⁴⁰⁰⁰ ₋₂₆₀₀	23.0 ± 5.4	2.5 ± 1.4

nucleon initiated events following the breakup of a heavy primary. The advantages of using such events are discussed in the references.^{12,16} Some of the energy determinations have been made by measuring the relative Coulomb scattering of the breakup fragments. Such measurements are more reliable than angular distribution methods.

Lohrmann, Teucher, and Schein¹² used scattering techniques and determined an arithmetic average energy of 250 GeV. However, since event multiplicities are increasing very slowly as a function of energy, perhaps as $\ln E$, a "logarithmic average energy" is more appropriate for comparison with multiplicity data. For these data we have calculated

$$\langle E \rangle = \exp(\ln E) = 170 \pm 50 \text{ GeV}.$$

It should be emphasized that this is not the average energy of the sample. It is, however, the value of the energy that should be used when discussing the dependence of the multiplicity on energy. We will show in the following section that this energy estimate is in agreement with the placement of these data on a plot of $\langle n_{ch} \rangle$ vs N_h .

The data of Rybicki and Wolter¹³ also represent breakup events. These authors based their energy determinations on the opening angles of the breakup fragments and obtained a value of 1 TeV. We have applied the correction factors $f(N_h)$ to the angular distributions presented by Rybicki and Wolter and averaged the logarithms of the energies to obtain an energy estimate of 510 ± 60 GeV.

For the breakup events from the ICEF¹⁵ and Brawley¹⁷ emulsion stacks the nucleon events from each breakup were assumed to be monoenergetic. Each track was corrected by the appropriate value of $f(N_h)$ and $\log_{10} \gamma_{c.m.}$ was calculated according to Eq. (3).

The event^{17,21,22} Brawley 1115 is particularly in-

teresting as it includes 20 nucleon collisions from the breakup of one heavy primary. Kim²¹ has determined the energy to be 570^{+70}_{-60} GeV using the relative scattering technique. Our angular distribution method gives 600 ± 150 GeV, in agreement with Kim's result, but substantially lower than earlier estimates. It should be pointed out that Brawley 1115 is included in the Rybicki and Wolter sample, and Kim's scattering measurement lends support to our energy estimate of that sample.

The primary-nucleon events of Barkow *et al.*¹⁴ and the ICEF collaboration¹⁵ exhibit similar properties and have been combined in our analysis. We have assumed that the entire sample represents primary-nucleon collisions in a narrow energy range above a detection threshold. Since the cosmic-ray flux falls off sharply with increasing energy, the distribution of Castagnoli energies is interpreted as a consequence of the statistical spread of Castagnoli energies rather than a significant actual energy spread. We have determined $\langle \log_{10} \tan \theta \rangle$ for each event from the published Castagnoli energy and calculated $\log_{10} \gamma_{c.m.}$ according to Eq. (3). These values were arithmetically averaged, weighting the values by their event multiplicities, and the energy calculated by Eq. (2). The value of $\langle \log \gamma_{c.m.} \rangle$ so obtained should be independent of N_h if our form for $f(N_h)$ is correct at these higher energies. The data shown in Table III are consistent with this criterion.

Ganguli and Malhotra¹⁸ have collected 88 primary-proton events of $N_h \leq 2$ for which they have estimated the energy at 10 TeV using the usual uncorrected Castagnoli estimate. Our approach reduces the energy estimate to 4.7 TeV. That this agrees with the energy estimate of the Barkow *et al.* and ICEF primaries is not surprising since about 40 of these events are included in the Ganguli and Malhotra sample.

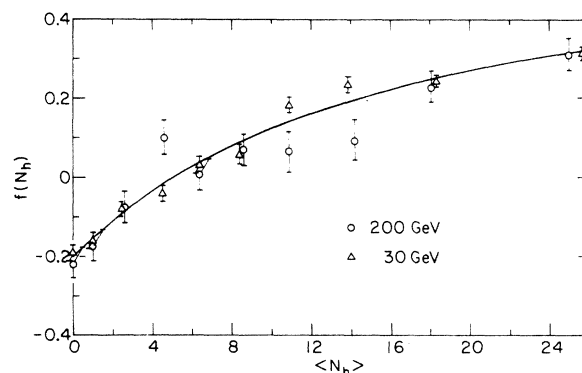


FIG. 1. A plot of the correction factor $f(N_h)$ as a function of N_h . The curve represents the best fit to the form given in Eq. (4). The parameters of this curve are given in Table I.

TABLE III. The values of $\langle \log_{10} \gamma_{c.m.} \rangle$ for the ICEF (Ref. 15) and the Barkow *et al.* (Ref. 14) cosmic-ray primary events as calculated for four N_h bins.

N_h bin	$\langle N_h \rangle$	$\langle \log_{10} \gamma_{c.m.} \rangle$
0-1	0.5	1.59 ± 0.08
2-4	3.0	1.69 ± 0.05
5-10	6.9	1.62 ± 0.08
≥ 11	16.7	1.79 ± 0.05
All	6.15	1.69 ± 0.03

C. $\langle n_{ch} \rangle$ vs N_h

An increase in the average charged multiplicity with N_h was noticed from the beginning of the study of collisions in emulsion.²³ Gibbs, Lord, and Goza⁴ pointed out that the increase was linear at 30 GeV and for certain cosmic-ray data.²⁴ This has recently been verified by our own data at 200 GeV and by the data of the Cracow group⁹ at 67 GeV and 200 GeV. Table IV shows our data at 30 GeV and 200 GeV. Figure 2 shows these data in a "double multiplicity" plot with the best-fit straight lines of Table V. Fits to a quadratic form are consistent with no curvature. Figure 3 shows cosmic-ray data with the best-fit straight lines. While these data are not as statistically significant as the accelerator data, the linearity still obtains.

In Fig. 4 we display the energy dependence of the slope and the intercept of the best straight-line fits to these data. We see that these parameters are consistent with a logarithmic increase with primary energy.

III. MODELS OF INTRANUCLEAR CASCADING

We have attempted to fit the double multiplicity data of Figs. 2 and 3 with model calculations of the IPM and CPM types. On the basis of the energy independence of the N_h distribution, we have assumed an energy-independent relation between

TABLE IV. $\langle n_{ch} \rangle$ as a function of N_h at 30 GeV and 200 GeV.

N_h	30 GeV		200 GeV	
	Events	$\langle n_{ch} \rangle$	Events	$\langle n_{ch} \rangle$
0	190	5.18 ± 0.18	26	9.58 ± 0.8
1	155	4.53 ± 0.26	23	9.87 ± 1.0
2-4	287	5.51 ± 0.20	} 68	12.8 ± 0.7
5-8	230	6.60 ± 0.22		
9-13	151	8.42 ± 0.31	} 51	16.9 ± 1.2
14-19	149	9.63 ± 0.34		
≥ 20	107	12.5 ± 0.4	13	24.4 ± 2.1
Total	1269	6.96 ± 0.12	181	13.9 ± 0.6

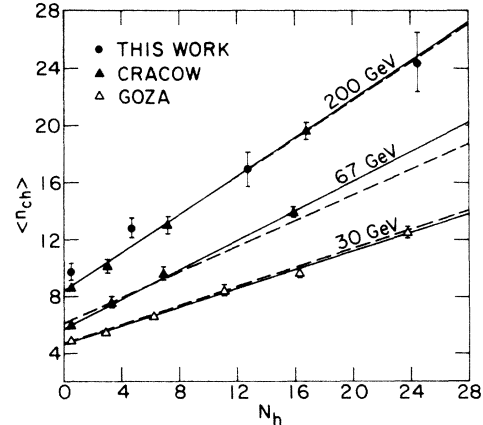


FIG. 2. The double multiplicity plot for the proton-emulsion data at accelerator energies. The solid lines are the best straight-line fits to each energy separately. The dashed lines represent the best simultaneous fit for our cascading model presented in Sec. III.

N_h and the average number of secondary interactions, η . This relation turns out to be linear since $\langle n_{ch} \rangle$ is linearly related to N_h and the models we have used relate $\langle n_{ch} \rangle$ to the number of interactions in a linear fashion.

The dependence on the number of interactions in the models of Fishbane and Trefil² has not yet been displayed, although presumably this dependence can be picked out of the computer calculations. We have generated a simplified IPM to build in a dependence on the number of secondary interactions. Our calculations are sufficiently close to those of the IPM of Fishbane and Trefil that we feel justified in letting them represent the IPM. Gottfried's energy flux cascade³ (EFC) also has an explicit dependence on the number of collisions and will be used to represent the CPM. Comparison with the Fishbane and Trefil models can be made by averaging over all N_h values, i.e., over all secondary interactions. Also these calculations have an explicit A dependence for which there is a smattering of data.

The fundamental input to all model calculations is the average proton-proton charged multiplicity, n_p . We have divided the multiplicity dependence into three regions with the following empirical forms:

$$n_p = 1.3(2m_p E + 2m_p^2)^{0.293}, \quad E \leq 10 \text{ GeV} \quad (5)$$

$$n_p = 1.75(2m_p E + 2m_p^2 - 10)^{0.25}, \quad 10 < E \leq 200 \text{ GeV} \quad (6)$$

$$n_p = -5.0 + 2.39 \ln E, \quad E > 200 \text{ GeV}. \quad (7)$$

In choosing form (7), we have fitted only to the accelerator data. All emulsion data are compared with the nuclear cascading models to be presented.

TABLE V. The best straight-line fits to the data of Fig. 2. See the text for a discussion of the two types of fit.

E (GeV)	Energy-independent fits	χ^2/DF	Energy-dependent fit	χ^2/DF
30	$(4.69 \pm 0.09) + (0.32 \pm 0.01)N_h$	0.53	$(4.69 \pm 0.07) + (0.34 \pm 0.01)N_h$	
67	$(5.79 \pm 0.09) + (0.51 \pm 0.01)N_h$	0.23	$(6.04 \pm 0.09) + (0.46 \pm 0.01)N_h$	1.2
200	$(8.45 \pm 0.18) + (0.66 \pm 0.03)N_h$	1.01	$(8.31 \pm 0.14) + (0.67 \pm 0.02)N_h$	

A. IPM calculations

In our model of the proton-nucleus interaction, the initiating interaction is pictured as occurring with a single constituent nucleon and assumed to have all the properties of a pure p -nucleon collision. The particles created in this primary collision can also interact before they leave the nucleus. Since at higher energy the number of secondary particles available to interact increases, our assumption that the number of secondary interactions, η , depends only on N_h means that the probability that a secondary will interact decreases with primary energy. Thus the effects of "shadowing" and "absorption" are built into the model in a simple way.

In order to calculate n_{ch} as a function of E and η , a number of additional assumptions are necessary. Created particles are assumed to be pions. The residual primary is viewed as retaining half of its incident energy, the remaining half to be equally divided among the pions. The residual primary nucleus and the secondary pions, charged

and neutral, have equal probabilities of interacting, and each collision produces exactly the average multiplicity n_p appropriate to its energy, subject to the constraint that final charge states reflect initial charge states. For example, a proton-neutron collision will produce one less final-state charged particle than a proton-proton collision. Only secondary collisions are considered.

In writing the complete expression for the average multiplicity $\langle n_{ch}(E, \eta) \rangle$ there are three terms corresponding to primary nucleon, residual primary nucleon, and secondary pion contributions. The first term is written in such a way that any interacting charged secondary particle is subtracted from the primary-collision contribution and included in its secondary-interaction term. This procedure prevents interacting charged particles from being counted in two of the terms. The two secondary-collision terms are written as products: the number of collisions of that type times the multiplicity per collision. The complete expression is

$$\begin{aligned} \langle n_{ch}(E, \eta) \rangle = & [n_p(E) - 0.5 - 0.67\eta] + \left\{ \frac{\eta}{1.5n_p(E) - 1.5} [n_p(0.5E) - 1.0] \right\} \\ & + \left\{ \frac{1.5n_p(E) - 2.5}{1.5n_p(E) - 1.5} \eta \left[n_p \left(\frac{0.5E}{1.5n_p(E) - 2.5} \right) - 1.0 \right] \right\}. \end{aligned} \quad (8)$$

The consequence of neglecting tertiary and higher-order interactions in the intranuclear cascade is to make Eq. (8) a linear function of η with energy-dependent coefficients:

$$\langle n_{ch}(E, \eta) \rangle = A(E) + B(E)\eta. \quad (9)$$

The experimental relationship discussed in Sec. IIC indicates that $\langle n_{ch}(E, N_h) \rangle$ is linearly related to N_h with energy-dependent coefficients:

$$\langle n_{ch}(E, N_h) \rangle = C(E) + D(E)N_h. \quad (10)$$

Setting Eqs. (9) and (10) equal leads to a linear relation between η and N_h ,

$$\begin{aligned} \eta(N_h) &= \frac{C(E) - A(E) + D(E)N_h}{B(E)} \\ &\equiv a + bN_h, \end{aligned} \quad (11)$$

where a and b are independent of the primary energy as discussed above.

To obtain the best values of a and b , we have substituted Eq. (11) into Eq. (9) obtaining

$$\langle n_{ch}(E, N_h) \rangle = A(E) + aB(E) + bB(E)N_h. \quad (12)$$

This form was fitted simultaneously to the data at 30, 67, and 200 GeV yielding

$$\eta(N_h) = (0.592 \pm 0.072) + (0.346 \pm 0.010)N_h, \quad (13)$$

with a χ^2 of 19.4 for 16 degrees of freedom.

The corresponding fits to Eq. (10) are compared in Table V with the best fits to the data at each energy separately and plotted in Fig. 2. While the simultaneous fit is in good agreement with the data at 30 and 200 GeV, it is only moderately good

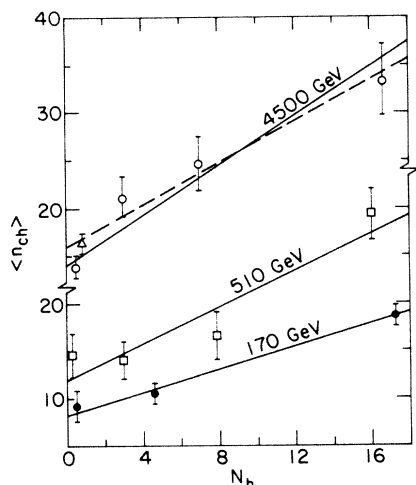


FIG. 3. Double multiplicity plot for the cosmic-ray data at 170 GeV (Ref. 12), 510 GeV (Ref. 13), and 4500 GeV (Refs. 14, 15, and 18). Also shown are the best-fit straight lines. The solid line at 4500 GeV is the fit to the Barkow *et al.* and ICEF points (open circles), while the dashed line uses the Ganguli and Malhotra point (open triangle) at small N_h .

at 67 GeV.

In order to compare our model with Fishbane's and Trefil's IPM, we have calculated $\langle n_{ch}(E, \langle N_h \rangle) \rangle$. This is our model prediction for the proton-emulsion charged multiplicity averaged over all N_h values. In Fig. 5 our result is compared with the result of Fishbane and Trefil and found to be nearly identical in the energy range of interest. The value $N_h = 7.0$ chosen for this calculation was a compromise between the value 7.2 obtained in our data at 30 and 200 GeV and the value 6.8 obtained from Eqs. (8) and (13) when $\langle n_{ch} \rangle$ is set equal to 12.9 ± 0.2 , the value obtained for 5500

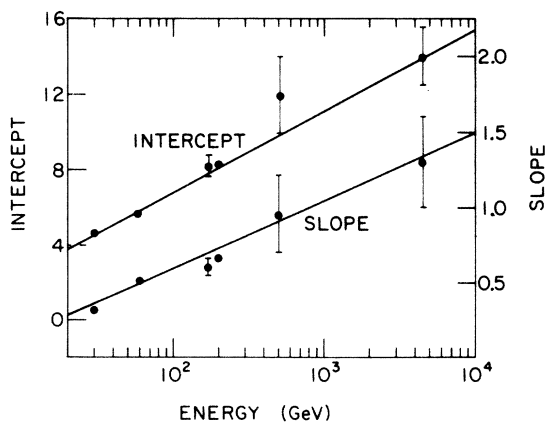


FIG. 4. The slopes and intercepts of the best-fit lines in Figs. 2 and 3 plotted against the primary energy. The slope and intercept are consistent with a logarithmic increase with energy.

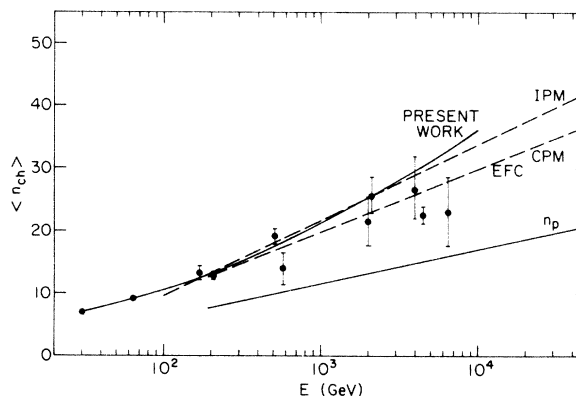


FIG. 5. Average n_{ch} in emulsion as a function of the incident energy. The cosmic-ray data are those of Table II. The accelerator data are from Refs. 7, 10, and 11. See the text for a discussion of the curves.

events at 200 GeV.¹¹

Also plotted on Fig. 5 are the calculations of the average charged multiplicity using Gottfried's EFC model and Fishbane's and Trefil's CPM. By normalizing these curves in the same manner, the two models give identical results. They are in better agreement with the data than the IPM. The curve for the multiplicity on hydrogen is shown for comparison.

Setting $N_h = \langle N_h \rangle = 7$ in Eq. (13) one calculates $\langle \eta \rangle = 3.1$. Therefore, on the average, the number of secondary collisions is small and it is reasonable to neglect tertiary terms. In Fig. 6 we show the model predictions compared with the cosmic-ray data. The fit is quite good at 170 GeV and 510 GeV, but rather poor at 4500 GeV. The 200 GeV line has been included to show that the data of

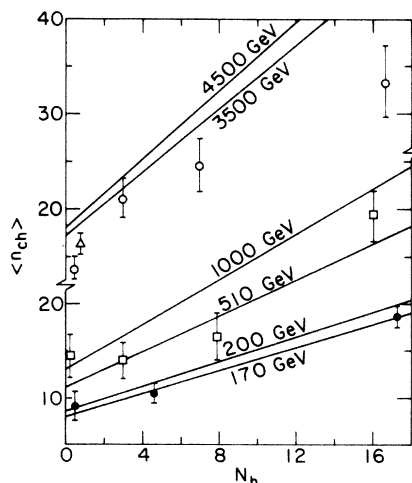


FIG. 6. Predictions for the double multiplicity relation at 170 GeV (●, Ref. 12), 510 GeV (□, Ref. 13), and 4500 GeV (○, Refs. 14 and 15, and △, Ref. 18) based on our IPM.

Lohrmann, Teucher, and Schein fall below this line instead of above, where it should have been for the published energy estimate of 250 GeV. This is in agreement with the logarithmic average energy we have used in Sec. II B to estimate the energy of this collection of events.

The difficulty at 4500 GeV cannot be corrected by assuming a lower value for the proton-proton multiplicity n_p at 4500 GeV as this would decrease the intercept but increase the slope, which is already too large. On the other hand, assuming a larger n_p decreases the slope but increases the intercept to an unreasonably large value.

The analysis of the high-energy cosmic-ray breakup events is quite consistent with these results. Although there are not enough interactions to create a reliable double multiplicity plot for these data, their average behavior can be compared with the model. In Table VI we compare the value of $\eta(\langle N_h \rangle)$ obtained from Eq. (13) with the value $\eta(\langle n_{ch} \rangle)$ obtained from Eq. (8) using the experimental values for $\langle N_h \rangle$, $\langle n_{ch} \rangle$, and E from Table II. These two values of η should agree if the model is correct. This is the case for $E \leq 500$ GeV. However, for $E > 1$ TeV, $\eta(\langle N_h \rangle)$ is consistently greater than $\eta(\langle n_{ch} \rangle)$. The model predicts too many particles at high energy.

B. The EFC model

Gottfried³ has cast his calculation of $\langle n_{ch} \rangle$ in the form

$$\langle n_{ch} \rangle = \frac{2}{3}n_p + \frac{1}{3}\nu n_p, \quad (14)$$

where ν is the *total* number of interactions and is independent of energy. Using the best-fit double multiplicity relation at 200 GeV from Table V, one then eliminates n_{ch} to obtain the result

$$\nu = (1.31 \pm 0.07) + (0.26 \pm 0.07)N_h. \quad (15)$$

Using Eqs. (14) and (15) and the forms (6) and (7) for n_p , one can calculate the double multiplicity relation at any energy. Since Gottfried's calcula-

tions are approximations for high energy, Eq. (14) should not hold for energies much below 200 GeV. In fact the calculations are in poor agreement with the data at 67 GeV. The disagreement is even larger at 30 GeV. The model fits the cosmic-ray data quite well and is substantially better than our IPM at 4500 GeV. (See Fig. 7.) The agreement is even better if the data on heavy primary breakup events are considered.

In Table VI we compare $\nu(\langle N_h \rangle)$ calculated from Eq. (15) and $\nu(\langle n_{ch} \rangle)$ calculated from Eq. (14) for all the cosmic-ray data. In contrast with the results of our IPM, the agreement in the ν values is excellent, especially considering the uncertainties in Eq. (15) and the proton-proton multiplicity at these energies.

In Gottfried's model the ratio R defined by

$$R = \frac{n_{ch}}{n_p} = \frac{2}{3} + \frac{1}{3}\nu \quad (16)$$

is independent of energy. For emulsion events¹¹ at 200 GeV one can use the bubble chamber²⁵ value $n_p = 7.68 \pm 0.11$ at 205 GeV to obtain $R = 1.68 \pm 0.03$, which yields $\langle \nu \rangle = 3.1$. Using the mean free path for hadrons in nuclear matter, Gottfried has calculated $\langle \nu \rangle$ directly and obtains $\langle \nu \rangle = 3.2$. Similarly, setting $N_h = 7$ in Eq. (15) one obtains $\langle \nu \rangle = 3.1$.

Using the data at 4500 GeV and Eq. (7) for n_p , one calculates $R = 1.5 \pm 0.1$ in agreement with the value at 200 GeV. At 170 GeV and 510 GeV one obtains the values $R = 1.78 \pm 0.12$ and $R = 1.9 \pm 0.1$, respectively.

Using Eqs. (15) and (16) one can calculate R for any value of N_h . We have decreased the energy estimate of the 88 events with $N_h \leq 2$ reported by Ganguli and Malhotra to 4700 GeV. For this sample $\langle N_h \rangle$ is approximately 0.8. The corresponding R calculated with Eq. (15) is 1.17 which compares favorably with the experimental value $R = 1.07 \pm 0.07$.

Figure 5 shows the calculated value of $\langle n_{ch} \rangle$ as a function of energy assuming $N_h = \langle N_h \rangle = 7$. In viewing this figure it is well to remember that the cos-

TABLE VI. Values of the parameter η based on our simplified version of the IPM and of the parameter ν based on the EFC model.

Reference	E (GeV)	$\eta(\langle n_{ch} \rangle)$	$\eta(\langle N_h \rangle)$	$\nu(\langle n_{ch} \rangle)$	$\nu(\langle N_h \rangle)$
12	170	3.5 ± 0.5	3.5 ± 0.1	3.3 ± 0.4	3.5 ± 0.6
ICEF 348	290	3.6 ± 1.2	3.9 ± 0.1	3.7 ± 0.9	3.8 ± 0.7
13	510	3.5 ± 0.4	3.1 ± 0.1	3.8 ± 0.4	3.2 ± 0.5
Brawley 1115	570	1.5 ± 0.9	2.4 ± 0.1	2.1 ± 0.8	2.6 ± 0.4
ICEF 23	2200	2.0 ± 0.9	2.7 ± 0.1	2.9 ± 0.9	2.9 ± 0.4
ICEF 16	2400	2.9 ± 0.7	7.5 ± 0.2	3.7 ± 0.7	6.5 ± 1.4
ICEF 33	4300	1.3 ± 1.0	2.7 ± 0.1	2.3 ± 1.0	2.9 ± 0.4
14 and 15	4500	1.5 ± 0.3	2.7 ± 0.1	2.5 ± 0.3	2.9 ± 0.4
18	4700	0.3 ± 0.2	0.9 ± 0.1	1.2 ± 0.2	1.5 ± 0.6
Brawley 1010	7800	1.1 ± 0.9	1.5 ± 0.1	2.2 ± 1.0	2.0 ± 0.2

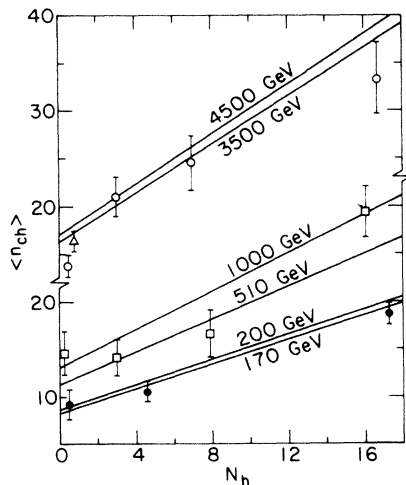


FIG. 7. Prediction for the double multiplicity relation at 170 GeV (●, Ref. 12), 510 GeV (□, Ref. 13), and 4500 GeV (○, Refs. 14 and 15, and △, Ref. 18) based on the EFC model.

mic-ray data have $\langle N_h \rangle < 7$, except for event ICEF 16.

Since $\langle \nu \rangle$ can be calculated as a function of the atomic number A of the nucleus, one can calculate the dependence of the average charged multiplicity on the atomic number. The data suitable for testing this A dependence are sparse, but do indicate a trend. Figure 8 shows data at 200 GeV for targets of hydrogen,²⁵ emulsion, and eight events in tungsten.²⁶ We and Hebert *et al.*²⁷ have further separated events in emulsion into interactions in the CNO group and the Ag-Br group. The data are quite suggestive of an $A^{1/3}$ dependence, although the statistical accuracy is not great. The EFC calculation agrees with the data quite well.

C. CPM

The CPM calculations of Fishbane and Trefil also yield an energy-independent ratio of n_{ch} to n_p . Their value also depends on the atomic number A of the nucleus and has the form

$$R = \frac{1}{2}(CA^{1/3} + 1). \quad (17)$$

The value of C is not well determined, but Fishbane and Trefil indicate that it is approximately 0.5. As shown in Fig. 8, this value underestimates the values of $\langle n_{ch} \rangle$. Using the value of R determined for our emulsion data, one calculates that $C = 0.66$. This curve is consistent with the data. The value of R obtained by Hebert *et al.* would give a value of $C = 0.59$. These curves are also displayed in Fig. 8.

IV. CONCLUSIONS

From the analysis of the data on proton-emulsion collisions which has been presented several general conclusions are evident. First, the data for the variables $\langle n_{ch} \rangle$, N_h , and $\langle \log \tan \theta \rangle$, for statistically meaningful samples, behave in a relatively simple and consistent manner from 30 GeV to 4500 GeV. Second, it has been demonstrated that all the data, as opposed to just $N_h = 0, 1$, are meaningful.

We have shown that the function $f(N_h) = \langle \log_{10} \tan \theta \rangle + \log_{10} \gamma_{c.m.}$ is independent of energy for data at 30 GeV and 200 GeV and is consistent with this result at 4500 GeV. Knowledge of $f(N_h)$ is useful in determining the energies of a sample of cosmic-ray events using the angular distribution method. However, the statistical fluctuations are still large, so that caution is urged for the interpretation of small samples of data. In particular, attempts to classify events energetically within a given sample of cosmic-ray interactions on the basis of the "Castagnoli energy," even with the corrections $f(N_h)$, are likely to be misleading.

By averaging the values of $\log \tan \theta$ as corrected by $f(N_h)$, we have concluded that the energies of cosmic-ray events are generally overestimated. A particularly important example is the group of events collected by Ganguli and Malhotra, which our analysis places at 4700 GeV, as compared with the original estimate of 10 000 GeV. At this lower energy these data are consistent with the $\ln E$ rise in the proton-proton multiplicity which pertains in the NAL and CERN ISR energy range.

We have found that the double multiplicity relation, $\langle n_{ch} \rangle$ vs N_h , is consistent with linearity from 30 GeV to 4500 GeV. The experimentally deter-

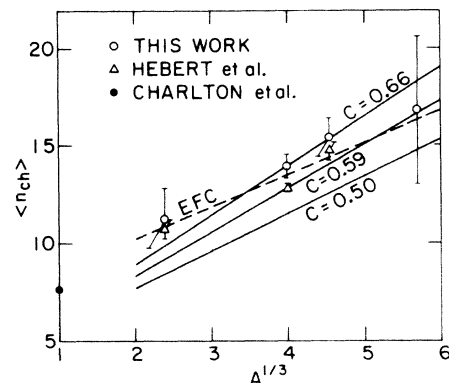


FIG. 8. Average charged multiplicity vs $A^{1/3}$ for 205-GeV protons in hydrogen and 200-GeV protons in emulsion and tungsten. The emulsion events have been separated into interactions in the CNO group and the Ag-Br group. The solid curves are the calculations using the CPM with various values of the parameter C [see Eq. (17)]. The dashed curve is that of the EFC model.

mined slopes and intercepts for these data increase with energy as $\ln E$.

Various models for intranuclear cascading have been compared with the experimental data. Each of the models involves a small number of collisions within the nucleus. Our IPM and the EFC model assume that the number of such collisions is independent of energy. Each of the models agrees with the accelerator data regarding the energy dependence of the average charged multiplicity. However, the IPMs predict too many particles at cosmic-ray energies.

Our IPM does not correctly give the parameters of the linear relation between $\langle n_{\text{ch}} \rangle$ and N_h at cosmic-ray energies, whereas, the EFC model does quite well.

The EFC model and the CPM (with an appropriate choice of the slope parameter) are both compatible with the dependence of the average charged multiplicity on the atomic number of the nucleus. The prediction of the Fishbane and Trefil IPM of an A -independent multiplicity for $A > 10$ is not compatible with the data.

In summary, we conclude that the data support the CPM and EFC descriptions of intranuclear cascading at these energies. Additional data at 400 GeV in emulsion and at a range of energies on nuclear targets are needed in order to further test and refine these models.

Note added in proof. Fishbane and Trefil²⁸ have formulated a dependence of n_{ch} on A which is considerably better than that discussed in Sec. III C and presented in Fig. 8. If the value of $(Q+R)$ in their Eq. (6.2) were set equal to 1.0, their curve would be consistent with the data.

ACKNOWLEDGMENTS

We express our gratitude to Dr. Lundy and Dr. Voyvodic as well as the NAL staff for making this experiment possible. We would also like to thank Dr. Furmanska, Dr. Gierula, and Dr. Slezak for providing us with their data at 67 and 200 GeV and Dr. Bali, Dr. Kotzer, and Dr. Trefil for valuable discussions.

*Research supported in part by the National Science Foundation, under Grant No. 39011.

¹A. Dar and J. Vary, Phys. Rev. D **6**, 2412 (1972).

²P. M. Fishbane and J. S. Trefil, Nucl. Phys. **B58**, 261 (1973); Phys. Rev. Lett. **31**, 734 (1973); SUNY Report No. ITP-SB-73-36, 1973 (unpublished).

³K. Gottfried, CERN Report No. TH 1735-CERN, 1973 (unpublished).

⁴R. E. Gibbs, J. J. Lord, and E. R. Goza, in *Proceedings of the Sixth Interamerican Seminar on Cosmic Rays, La Paz, Bolivia, 1970* (Universidad Mayor de San Andrés, La Paz, 1970), Vol. 41, p. 1019.

⁵R. Hołyński, S. Krzywdziński, and K. Zaleswski (unpublished).

⁶J. Babecki, Z. Czachowska, B. Furmanska, J. Gierula, R. Hołyński, A. Jurak, S. Krzywdziński, G. Nowak, B. Slezak, and W. Wolter (unpublished).

⁷E. R. Goza, thesis, University of Washington, 1962 (unpublished).

⁸ n_{ch} refers to the number of charged particles emitted in a proton-nucleus collision. It is sometimes called n_s in the literature.

⁹B. Furmanska and B. Slezak, private communication, 1973.

¹⁰J. Babecki, J. Z. Czachowska, B. Furmańska, J. Gierula, R. Hołyński, A. Jurak, S. Krzywdziński, G. Nowak, B. Slezak, and W. Wolter, Phys. Lett. **47B**, 268 (1973).

¹¹J. Hébert *et al.*, Barcelona-Batavia-Belgrade-Bucharest-Lund Lyon-McGill-Nancy-Ottawa-Paris-Quebec-Rome-Valencia Collaboration, *Experiments on High Energy Particle Collisions—1973*, proceedings of the international conference on new results from experiments on high energy particle collisions, Vanderbilt

University, 1973, edited by Robert S. Panvini (A.I.P., New York, 1973); in *Proceedings of the Fifth International Conference on High Energy Physics and Nuclear Structure*, Uppsala, Sweden, 1973 (unpublished).

¹²E. Lohrmann, M. Teucher, and M. Schein, Phys. Rev. **122**, 672 (1961).

¹³K. Rybicki and W. Wolter, Polish Institute of Nuclear Research, Report "P" No. 1127/VII/PH (unpublished).

¹⁴A. G. Barkow, B. Chamany, D. M. Haskin, P. L. Jain, E. Lohrmann, M. W. Teucher, and M. Schein, Phys. Rev. **122**, 617 (1961).

¹⁵ICEF Collaboration, Brisbout *et al.*, Nuovo Cimento Suppl. Series I, **1**, 1039 (1963).

¹⁶M. Koshiba, C. H. Tsao, C. L. Deney, R. Fricken, R. W. Huggett, B. Hildebrand, R. Silberberg, and J. Lord, Nuovo Cimento Suppl. Series I, **1**, 1091 (1963).

¹⁷M. Koshiba, in *Proceedings of the Eighth International Conference on Cosmic Rays, Jaipur, India, 1963*, edited by R. R. Daniel *et al.* (Commercial Printing Press, Bombay, India, 1964). Brawley 1115 is also discussed in Refs. 21 and 22.

¹⁸S. N. Ganguli and P. K. Malhotra, Phys. Lett. **42B**, 83 (1972).

¹⁹H. Meyer, M. W. Teucher, and E. Lohrmann, Nuovo Cimento **28**, 1399 (1963).

²⁰C. Castagnoli, G. Cortini, D. Moreno, C. Franzinetti, and A. Manfredini, Nuovo Cimento **10**, 1539 (1953).

²¹C. O. Kim, Phys. Rev. **158**, 1261 (1967).

²²F. Abraham *et al.*, Phys. Rev. **159**, 1110 (1967).

²³H. Winzeler, Nucl. Phys. **69**, 661 (1965).

²⁴Obviously this is closely related to the observation of Refs. 19 and 23 that $\langle N_h \rangle$ is linearly related to n_{ch} .

²⁵G. Charlton *et al.*, Phys. Rev. Lett. **29**, 515 (1972).

²⁶J. R. Florian, L. D. Kirkpatrick, J. J. Lord, J. Martin,

R. E. Gibbs, P. Kotzer, and R. Piserchio, *Particles and Fields—1973*, edited by H. H. Bingham, M. Davier, and G. R. Lynch (A.I.P., New York, 1973).

²⁷J. Hebert *et al.*, Barcelona-Batavia-Belgrade-

Bucharest-Lund-Lyon-McGill-Nancy-Ottawa-Paris-Quebec-Rome-Valencia collaboration (unpublished).

²⁸P. M. Fishbane and J. S. Trefil, *Phys. Rev. D* **9**, 168 (1974).

Measurement of the magnetic moment and of the decay parameters of the Ξ^- hyperon*

R. L. Cool,† G. Giacomelli,‡ E. W. Jenkins,§ T. F. Kycia,

B. A. Leontic,|| K. K. Li, and J. Teiger¶

Brookhaven National Laboratory, Upton, New York 11973

(Received 24 April 1974)

A measurement of the magnetic moment and of the decay parameters of the Ξ^- hyperon is reported. The measurement gave $\mu_{\Xi} = (-2.1 \pm 0.8)$ nuclear magnetons, corresponding to a gyromagnetic ratio of $g_{\Xi} = 4.2 \pm 1.6$. The measured Ξ^- decay parameters are $\alpha_{\Xi} = -0.39 \pm 0.05$, $\beta_{\Xi} = 0.08 \pm 0.26$, $\gamma_{\Xi} = 0.92 \pm 0.03$ ($\phi_{\Xi} = 5^\circ \pm 16^\circ$); and the lifetime $\tau_{\Xi} = (1.637 \pm 0.050) \times 10^{-10}$ sec. In the accepted angular range for the production of the Ξ^- (about $4.2^\circ < \theta_{\text{lab}} < 11.5^\circ$) in the reaction $K^- + p \rightarrow K^+ + \Xi^-$, the polarization of the Ξ^- is 0.29 ± 0.10 , 0.44 ± 0.09 , 0.36 ± 0.10 , and 0.21 ± 0.06 at laboratory momenta of 1.74, 1.80, 1.87, and 1.83 GeV/c, respectively.

I. INTRODUCTION

The measurement of the magnetic moment of a particle can provide a test of the validity of a theory. Such tests have been applied to quantum electrodynamics by measuring the magnetic moments of the electron and of the muon. The agreement between theory and experiment was found to be quite striking.

The magnetic moments of the baryons can be used to test the validity of the strong-interaction theories, in particular of unitary-symmetry theories. They could also give evidence for or against the various models for the fundamental triplets. Figure 1 shows the members of the $\frac{1}{2}^+$ baryon octet. SU(3) symmetry predicts that, apart from mass corrections, the members of the various U -spin multiplets have the same magnetic moment. The relation among the magnetic moments of the octet is given by¹

$$\mu = \mu_2 - \mu_1 Q - \mu_2 [U(U+1) - \frac{1}{4}Q^2], \quad (1)$$

where Q is the charge and U is the U -spin. μ_2 and μ_1 may be determined from the known magnetic moments of the proton μ_p and of the neutron μ_n as

$$\mu_p = \frac{1}{2}\mu_2 - \mu_1 \quad (2)$$

and

$$\mu_n = -\mu_2. \quad (3)$$

As a consequence, (1) predicts the values of the

magnetic moments of the other members on the octet. In particular, the magnetic moment of the Ξ^- hyperon in units of nuclear magnetons ($\mu_N = e\hbar/2m_p c = 3.153 \times 10^{-18}$ MeV/c) is then predicted to be

$$\begin{aligned} \mu_{\Xi} &= -(\mu_n + \mu_p) \\ &= -0.88\mu_N. \end{aligned} \quad (4)$$

The method of measuring the magnetic moment of the Ξ^- is that of determining the angle of precession of the Ξ^- polarization vector after passing through a strong magnetic field.² The Ξ^- hyperons are produced in the reaction

$$K^- + p \rightarrow \Xi^- + K^+, \quad (5)$$

which acts as the polarizer. The polarization vector is perpendicular to the plane of production of the Ξ^- and therefore perpendicular to the Ξ^- direction.

The Ξ^- passes through a strong magnetic field which is essentially parallel to the Ξ^- momentum and therefore perpendicular to the Ξ^- magnetic moment (see Fig. 2). With this arrangement the Ξ^- track does not curve appreciably in the magnetic field.

In the Ξ^- rest frame the equation of motion of the polarization vector $\hat{\sigma}_{\Xi}$ in a magnetic field \vec{H} is

$$\frac{d\hat{\sigma}_{\Xi}}{dt} = \frac{\mu_{\Xi}}{s_{\Xi}\hbar} \hat{\sigma}_{\Xi} \times \vec{H}, \quad (6)$$

where μ_{Ξ} and $s_{\Xi}\hbar$ are respectively the magnetic moment and the spin of the Ξ^- . By integrating